ZIBELINE INTERNATIONAL™ PUBLISHING

ISSN: 2521-2893 (Print)
ISSN: 2521-2907 (Online)
CODEN: ESPADC

Earth Sciences Pakistan (ESP)

DOI: http://doi.org/10.26480/esp.01.2024.05.18

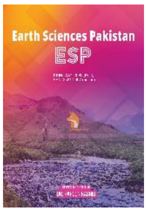

CrossMark

RESEARCH ARTICLE

GROUND WATER SUSTAINABILITY IN A CRYSTALLINE ROCK ENVIRONMENT USING ELECTRICAL RESISTIVITY AND MCDA APPROACH IN THE FEDERAL POLYTECHNIC ADO-EKITI, EKITI STATE, NIGERIA

Bawallah Musa Adesola[a], Adebayo Ayodele Emmanuel[b], Ilugbo Stephen Olubusola[c*], Adewumi Olajumoke Abisola[b], Ayodele Tola[c], Olutomilola Olabode Olusola[d]

[a]Department of Applied of Geophysics, Federal University of Technology Akure, Nigeria
[b]Department of Minerals and Petroleum Resources Engineering Technology, Federal Polytechnic Ado Ekitit, Ekiti State, Nigeria
[c]Department of Physics, Lead City University Ibadan, Nigeria
[d]Department of Geology, Afe Babalola University, Ado Ekiti, Nigeria
**Corresponding Author Email: ilugbo.stephen@lcu.edu.ng*

ARTICLE DETAILS

Article History:

Received 20 February 2024
Revised 15 March 2024
Accepted 01 April 2024
Available online 03 April 2024

ABSTRACT

Extensive growth in development, urbanization, and population has exacted more pressure on the availability and quality of groundwater resources. Human effort has been directed at solving groundwater scarcity in a crystalline basement rock environment, through the identification of joints, cracks, fractures, faults, and weathered materials that may exhibit favourable disposition to groundwater accumulation for water sustainability. This research applied Multi-Criteria Decision Analysis (MCDA) in the context of Analytical Hierarchical Process (AHP) to geoelectric parameters to model Groundwater Potential Zones (GWPZ) in the Federal Polytechnic, Ado Ekiti, Ekiti State, Nigeria. The Electrical Resistivity method was adopted using 2D Resistivity Tomography and Vertical Electrical Sounding (VES) utilizing Schlumberger configuration. 2D Resistivity Tomography was delineated to determine vertical and lateral ranges in apparent resistivity of the subsurface geological properties favourable to groundwater accumulation and development. Eight (18) VES were acquired across the study area. The iterated VES results were used to generate geoelectric sections, maps, and second-order parameters. The MCDA in the context of the AHP technique was used to assign scores to various contributing parameters based on their relative contribution to groundwater potential. The GWPZ was generated by incorporating the selected and weighting seven important defined variables (Coefficient of anisotropy, overburden thickness, aquifer resistivity, aquifer thickness, storativity, transmissivity, and hydraulic conductivity) in the Surfer 12 environment in reflection to their groundwater availability. The groundwater potential was categorized into high, moderate, low, and very low. Very low to low groundwater potential characterized the entire study area, occupying 75% with moderate to high occupying 25%. The finding revealed that the study area was characterized by very low to low groundwater potential. This research will assist in the development and monitoring of groundwater occurrences by decision policymakers to improve recharge techniques, especially in very low and low groundwater recharge zones.

KEYWORDS

Groundwater sustainability, MCDA, AHP, Geo-factors, Ado

1. INTRODUCTION

The Earth's subsurface has become the safest and most abundant source of potable water in comparison to the Earth's surface as it is often shielded from direct human activities (Ilugbo and Adebiyi, 2017; Abijith *et al.*, 2020). However, any undetected contamination of this resource poses a threat to the well-being and continued existence of man in the environment (Ilugbo et al., 2018a; Adebo et al., 2018; Adebiyi et al., 2018; Akinluyi, et al., 2018, 2021; Bawallah et al., 2021a). Groundwater is one of the most valuable natural resources on the earth's surface and serves as one of the main sources of drinking water (Boobalan and gurugnanam, 2016; Ilugbo et al., 2018b; Adebo et al., 2022; Olubusola et al., 2023). Basement complex has a problem with potable groundwater supply due to the crystalline nature of the underlying rock which lacks primary porosity (Adebo et al., 2019; Ilugbo et al., 2020, Bawallah et al., 2021b, Olubusola et al., 2023). Groundwater storage capacity in those areas is dependent on the depth of weathering and intensity of fracturing of the underlying rock (Abu El-Magd and Embaby, 2021; Anusha et al., 2022). For basement complex rocks to become good aquifers, they must be highly fractured and highly weathered (Ilugbo et al., 2018c; Bawallah et al., 2021a). In the basement complex, groundwater normally occurs in the porous and permeable substrate which is an underground layer of water-bearing permeable rock or unconsolidated materials such as gravel, sand, confined by impermeable confining bedrock such as shale (Ilugbo et al., 2019; Bawallah et al., 2020a; Akintorinwa et al., 2020). It is however more prominent within the weathered and fractured basement where it could either be confined by overlying impermeable and highly resistive rocks or remain unconfined but trapped by the low permeable and highly resistive fresh basement (Bawallah et al., 2020b; Al-Djazouli et al., 2020; Ilugbo et al., 2020). The thickness of the weathered overburden and fractured zone determined the nature and intensity of hydrodynamic activities within the usually discrete bodies of an aquifer in the terrain (Bawallah et al., 2021).

In typical basement complex areas such as the study area, the occurrence of groundwater in recoverable quantity as well as its circulation, are controlled by geological factors i.e. faults, joints, and fracture zones (Ilugbo

Quick Response Code	Access this article online	
	Website: www.earthsciencespakistan.com	**DOI:** 10.26480/esp.01.2024.05.18

Cite the Article: Bawallah Musa Adesola, Adebayo Ayodele Emmanuel, Ilugbo Stephen Olubusola, Adewumi Olajumoke Abisola, Ayodele Tola, Olutomilola Olabode Olusola (2024). Ground Water Sustainability in A Crystalline Rock Environment Using Electrical Resistivity and Mcda Approach in The Federal Polytechnic Ado-Ekiti, Ekiti State, Nigeria. *Earth Sciences Pakistan, 8(1): 05-18.*

et al., 2018b; Bawallah et al., 2018a). The delineation of these features is essential for a better understanding of the subsurface geology of these areas in terms of their groundwater potential (Paul et al., 2020). Therefore to target potential basement aquifers that provide a copious supply of groundwater in these areas, the aforementioned geologic features must be intercepted by boreholes (Bawallah et al., 2018b; Aggarwal et al., 2019; Oyedele, 2019; Ilugbo et al., 2023). Thus, the groundwater potential of a basement complex area is determined by a complex interrelationship between the geology, post-emplacements, tectonic history, weathering processes, and depth, the composition of the weathered layer, aquifer types, and combination, groundwater flow pattern, climate, recharge, and discharge processes (Olorunfemi, 2008).

To produce a groundwater potential map of higher reliability and precision in a given study area, the effects of all the important parameters (geoelectric and geologic) that can contribute to the groundwater occurrence in the area must be integrated (Tolche, 2021; Sengupta et al., 2021; Pande et al., 2022). However, the methodology of integrating these parameters, such that the relative importance of each is reflected, is still a challenge that has not been efficiently handled within the investigated area. Since our major tools in this research are to produce prediction model maps for local scale analysis, this study additionally explored the potential of the surfer software using Multi-Criteria Decision Analysis (MCDA) to produce predictive models with unbiased prediction in the study area. The principle of Multi-Criteria Decision Analysis (MCDA) in the context of the Analytical Hierarchy Process (AHP) approach is proposed as a technique that can yield a prediction model of higher reliability and precision (Mohammadi-Behzad et al., 2019; Tanveer et al., 2020; Saranya and Saravanan, 2020). The proposed technique is applied to geoelectric and geologic parameters derived from electrical resistivity methods to evaluate groundwater resources. The advantage of the proposed technique is that it reduces bias in decision-making because it provides a useful mechanism for checking the consistency of the evaluation measures and alternatives suggested by experts (Arshad et al., 2020; Olubusola et al., 2023; Ozegin et al., 2023). The need to effectively represent and quantify uncertainties in a model groundwater resource which was difficult to assess by the most used data mining techniques is a knowledge gap to be filled in the field of groundwater research domains. The mostly used GIS-GRA (General Rating Approach) methods in groundwater resources have limitations in the quantification of uncertainties associated with subsurface parameters relevant in groundwater resource prediction (Al-Djazouli et al., 2020). The quest for employing a modeling method that can accommodate the expert's input for the appropriate handling of such geoelectric parameters series of uncertainties is an intention in this study. By Raje and Mujumdar (2010), the types of uncertainty that are associated with these data sets are stochastic uncertainty and systemic uncertainty. These uncertainty types require modeling techniques that can manage them efficiently to enhance accuracy in prediction. This is because such uncertainties often have significant impacts on modeling results which sometimes lead to inaccurate outcomes and undesirable consequences if not properly handled (Feizizadeh et al., 2014).

Hence, this research proposes Multi-Criteria Decision Analysis (MCDA) in the context of the Analytical Hierarchy Process (AHP) approach as a prediction model to resolve this limitation and production of a more accurate and reliable groundwater resource prediction model viable for decision-making in the study area.

1.1 Site Description And Geology Of The Study Area

The current study was conducted in Nigeria's southwestern region, as shown in Figure 1. The research region is characterized UTM by Easthing coordinates ranging from 753830 to 754130 E and Northing coordinates spanning from 839500 to 839750 N. The examined region is characterized by higher elevations in the northern and northwestern regions and lower elevations in the southern parts. The elevations reported within the research zone range from 93 to 362 m, above the mean sea level (datum). The research region falls within the southwestern crystalline basement complex rock of Nigeria (Rahaman, 1988). Ekiti State is characterized by granite gneiss, charnockite baxlite charnockitic rock, granite, granodorite biotite hornblende, older granite, quartzite kyante schistose quartzite, undifferentiated metasediment schist, and migmatite gneiss (Olarewaju, 1988; Aluko, 2008). The research region falls within older granite rock.

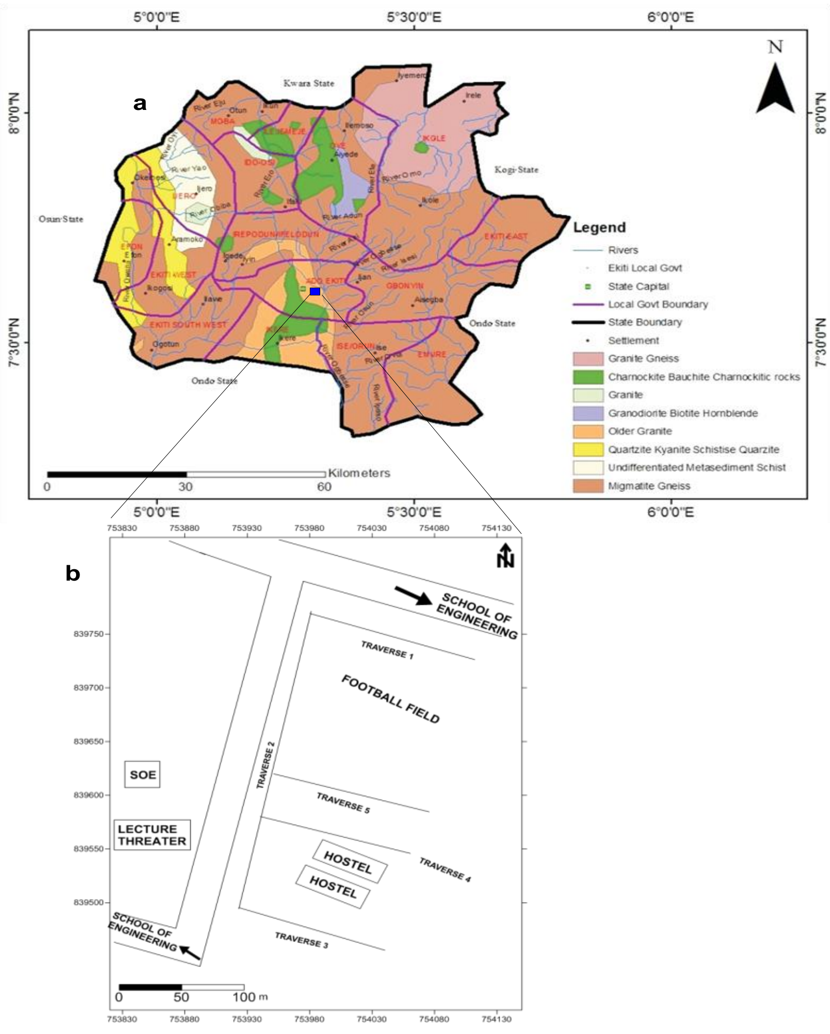

Figure 1: (a) Geological Map of Ekiti State Showing the Study Area (after Ademilua, 1997) (b) Study Location Map

Cite the Article: Bawallah Musa Adesola, Adebayo Ayodele Emmanuel, Ilugbo Stephen Olubusola, Adewumi Olajumoke Abisola, Ayodele Tola, Olutomilola Olabode Olusola (2024). Ground Water Sustainability in A Crystalline Rock Environment Using Electrical Resistivity and Mcda Approach in The Federal Polytechnic Ado-Ekiti, Ekiti State, Nigeria. *Earth Sciences Pakistan, 8(1): 05-18.*

2. Methodology

Five traverses were established across the investigated area in approximately E-W orientation (Figure 2). The electrical resistivity was engaged using 2D Resistivity Tomography and Vertical Electrical Sounding (VES) utilizing Schlumberger arrays. The 2D resistivity tomography was acquired along traverses one to three with 5 m inter-electrode spacing while the expansion factor for the inter-dipole varied from 1-5, to delineate both vertical and lateral ranges in apparent resistivity of the subsurface geological properties. The Pasi resistivity meter was used to obtain the resistivity readings. The data obtained were incorporated into 2D images of the subsurface using the DIPPRO™ 4.0 software inversion (Dippro, 2000). Eighteen (18) VES data points were established and acquired along the five traverses with (AB/2) current electrode spacing of 200 m. The apparent resistivity values obtained were plotted against the electrode spread (AB/2). A Partial curve matching approach was applied to interpret the data quantitatively with aids of computer-assisted 1-D forward modeling using WinResist 1.0 version software (Vander Velpen, 2004). The results obtained from the iterated VES curves were used to generate geoelectric sections, maps, and second-order parameters.

The Dar-Zarrouk parameters are obtained from the first-order parameters (geoelectric parameters) which are Total longitudinal unit conductance (S), Total transverse unit resistance (T), and coefficient of anisotropy (λ) using these mathematical expressions.

$$s_i = \Sigma \frac{hi}{\rho i} \quad 1$$

$$T_i = \Sigma h_i \rho_i \quad 2$$

$$\rho_I = \Sigma \frac{Ti}{hi} \quad 3$$

$$\rho_L = \Sigma \frac{hi}{Si} \quad 3$$

$$\lambda = \sqrt{\frac{\rho I}{\rho L}} \quad 4$$

Si = Total longitudinal unit conductance, Ti = Total transverse unit resistance, Hi = Layer thickness, ρi = Layer resistivity, ρt = Transverse resistivity, ρL = Longitudinal resistivity,

n = number of layers, λ = coefficient of Anisotropy.

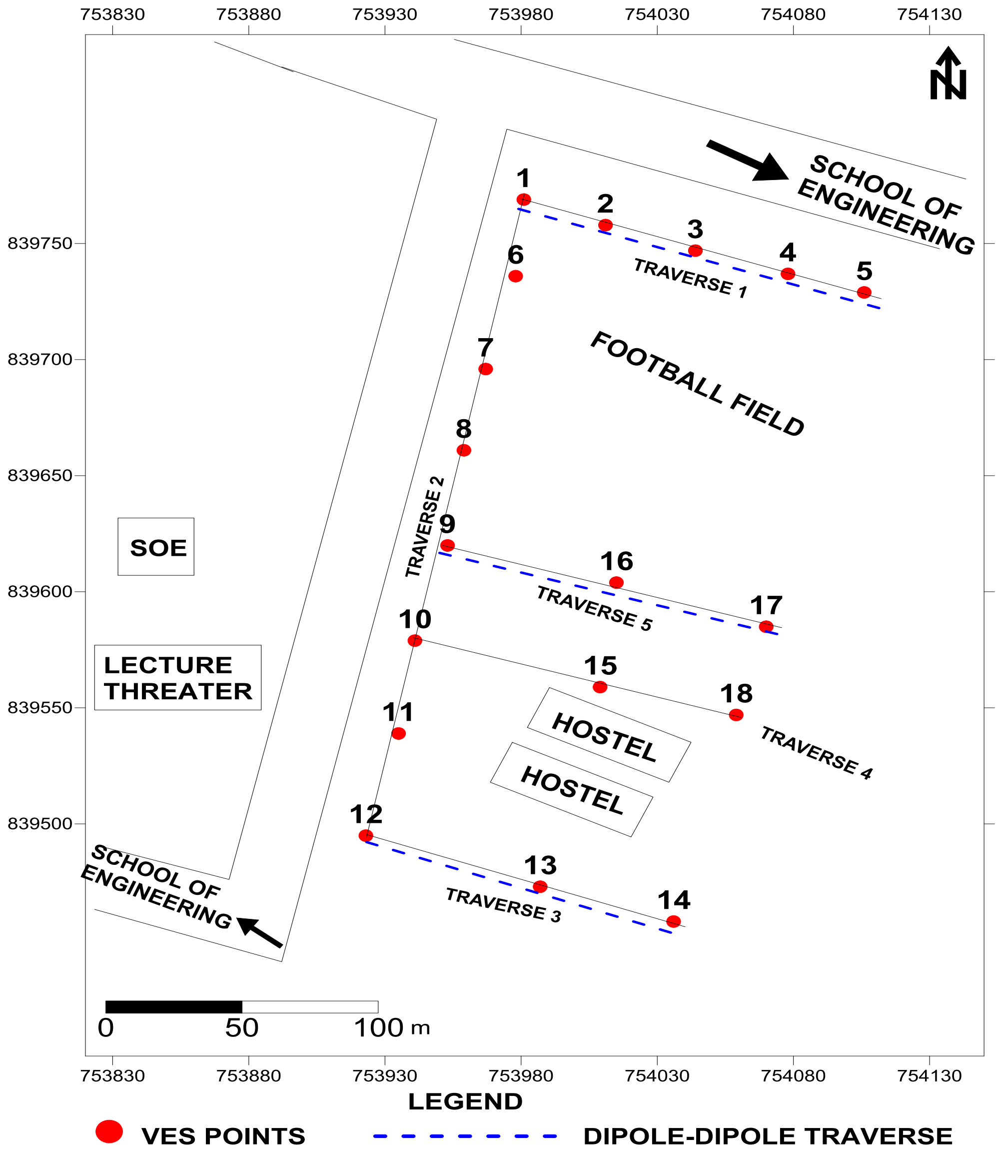

Figure 2: Data Points Map of the Study Area

The degree of inhomogeneity, expressed as electrical coefficient of anisotropy (λ), correlates linearly with groundwater yield; Hence, Y = f (λ).

Whereas,

$$K = 0{:}0538e^{-0.0072\rho} \quad 5$$

where:

K = Hydraulic Conductivity (m/s)

ρ = Apparent Resistivity

$$T = Kb \quad 6$$

where:

T = Transmissivity (m^2/s)

K = Hydraulic Conductivity

b = Aquifer Thickness

Storativities have received even less attention than specific yield. The sole estimation technique in popular circulation appears to be the 'rule of thumb', in which it is claimed that since storativity (S) varies directly with aquifer thickness (b), then the relation:

$$S = 3\,x'10^{-6}b \qquad 7$$

S = Storativity

b = Aquifer Thickness

Seven parameters was subjected to statistical analysis using Multi-Criteria Decision Analysis (MCDA) in the context of Analytical Hierarchy Process (AHP).

The groundwater occurrence parameters for pairwise ranking and weighting were developed using AHP.

2.1 Multi-Criteria Evaluation Techniques (MCDA)

2.1.1 Pairwise comparison/Construction of Pairwise Comparison Matrix

To evaluate groundwater occurrences for decision-makers MCDA in the context of AHP is widely engaged (Satty 1980). All the criteria were compared with one another to determine the weight and rank of each parameter using AHP which is based on the series construction of pairwise comparison matrices (Satty 1980). The geometric mean and normalized weight were measured through the assessment of many datasets in a comparison matrix using AHP techniques. According to the expert opinion and field experience for groundwater occurrence impact, the weights for each parameter were assigned and integrated. The parameter that influences directly to groundwater was assigned a high weightage while the parameter that influenced indirectly to groundwater was assigned a low weightage due to the cluster relationship among all parameters in the study area. In this regard, the seven (7) thematic layers were used to generate the pairwise comparison matrix (Table 1). Table 2 illustrates the rank and weights of each parameter. Inconsistency may occur in the weighting of the parameter, because pairwise comparison is carried out using personal judgments. There is a need to determine the consistency of the judgments through the Consistency Verification Operation (CVO). The CVO is one of the merits of the AHP approach, and is engaged to determine the degree of consistency of the judgments by estimating the Consistency Ratio (CR). The inverse numbers of the upper diagonal were utilized to generate the comparison matrix's lower triangular matrix.

Therefore, if aij is a component of the matrix's row i and column j, equation 1 is applied to complete the bottom diagonal;

$$a_{ij} = 1/a_{ij} \qquad 1$$

Table 1 displays the matrix with the lowest diagonal.

Table 1: groundwater potential zonation paired-wise comparison matrix

		A	B	C	D	E	F	G
CA	**A**	1	5	5	5	5	5	5
OT	**B**	1/5	1	3	3	3	3	3
AR	**C**	1/5	1/3	1	3	3	3	3
AT	**D**	1/5	1/3	1/3	1	3	3	3
S	**E**	1/5	1/3	1/3	1/3	1	3	3
T	**F**	1/5	1/3	1/3	1/3	1/3	1	3
HC	**G**	1/5	1/3	1/3	1/3	1/3	1/3	1
TOTAL		2.20	7.67	10.33	13.00	15.67	18.33	21.00

2.2 Calculation of Multi-criteria Evaluation Techniques (MCDA)

Weights were assigned to the parameters using the technique of MCDA. MCDA is a technique that allows map layers to be weighted to reflect their relative influence or importance (Kardi, 2006). The best set of weights for each index was produced by computing the Eigenvectors. This was achieved by computing the sum of the value in each column of the pairwise comparison matrix, then normalizing the matrix by dividing each element in the matrix by its column total, and finally computing the average of the elements in each row of the normalized matrix (Table 2). These averages give an estimate of the relative weights of the parameter being compared. The final weightings for the factors are the normalized values of the eigenvectors that are associated with the maximum Eigenvalues of the ratio (reciprocal) matrix. This procedure is the best way to minimize the impact of inconsistencies in the ratios. The relative weights of the criteria are shown in Table 3. The prevailing geological factors and recharge mechanisms characterizing the area of study.

Table 2: Calculation of the Criteria Weights for Groundwater Recharge Potential

	CA (j=1)	OT (j=2)	AR (j=3)	AT (j=4)	S (j=5)	T (j=6)	HC (j=7)	ΣWij
CA (i=1)	0.46	0.65	0.48	0.39	0.32	0.27	0.24	2.81
OT (i=2)	0.09	0.13	0.29	0.23	0.19	0.16	0.14	1.23
AR (i=3)	0.09	0.04	0.10	0.23	0.19	0.16	0.14	0.95
AT (i=4)	0.09	0.04	0.03	0.08	0.19	0.16	0.14	0.73
S (i=5)	0.09	0.04	0.03	0.03	0.06	0.16	0.14	0.55
T (i=6)	0.09	0.04	0.03	0.03	0.02	0.05	0.14	0.40
HC (i=7)	0.09	0.04	0.03	0.03	0.02	0.02	0.05	0.28
	1	1	1	1	1	1	1	**ΣWij/Σj = 1**

CA – Coefficient of anisotropy, OT – Overburden Thickness, AR – Aquifer Resistivity, AT – Aquifer Thickness, S – Storativity, T – Transmissivity, HC – Hydraulic Conductivity.

2.2.1 Examination of the Consistency of the Pairwise Matrix

Because the comparisons were carried out through personal or subjective judgments, some degree of inconsistency and bias may occur. To guarantee some levels of consistency in the judgments, consistency verification is done to check the logical consistency of the pairwise matrix. The computation of the consistency ratio (CR) is used to do consistency verification. Consistency verification is one of the most important of the AHP. Consistency ratio (CR) is the ratio of consistency index (CI) to random index (RI). Generally, if CR is less than or equal to 0.1, the judgments are consistent, so the derived weights can be used. CR is estimated using the following steps.

(i) Multiply each column of the pairwise comparison matrix, A by the corresponding weight, W.

$$AW = \begin{bmatrix} 1 & a_{12} & a_{13} & \dots & a_{1n} \\ 1/a_{21} & 1 & a_{23} & \dots & a_{2n} \\ 1/a_{31} & 1/a_{32} & 1 & \dots & a_{3n} \\ & & & & \\ 1/a_{n1} & 1/a_{n2} & 1/a_{n3} & \dots & 1 \end{bmatrix} \begin{bmatrix} w_1 \\ w_2 \\ w_3 \\ \\ w_n \end{bmatrix}$$

(ii) Calculate the largest Eigen value, λ_{max} for matrix A;

$$\lambda_{max} = \frac{1}{n}\Sigma(\Sigma ni = \frac{1 \text{ row entry of Aw}}{\text{ith entry of row}}) \qquad 3$$

(iii) Calculate the consistency index (CI);

$$CI = \frac{\lambda max - n}{n-1} \qquad 4$$

where n = number of criteria used

(iv) Lastly, calculate the consistency ratio, CR,

$$CR = \frac{CI}{RI} \qquad 5$$

where RI, the random index, is calculated using the following equation:

$$RI = \frac{\lambda max - n}{n-1} \lambda max\,(n) \qquad 6$$

From the expression for CI shown above, the more the value of λ_{max} is approaching the n value, the more the matrix becomes more consistent. A perfect consistent level is reached when the consistency measure (λ_{max}) is equal to n. Therefore, when the matrix is perfectly consistent, CI = 0, hence CR = 0. If CR < 0.1 (10 %), then the comparison values are still considered consistent (Saaty, 1980). On the other hand, if CR > 0.1, then the entry values are not consistent, and the pairwise comparison matrix has to be reconstructed.

To check for the groundwater potential weighting consistency, λ_{max} is the average value of the consistency vector;

Where λ_{max} = 7.2201, CI = 0.03668 (using equation 4) and for n = 7, RI = 1.34

$$CR = \frac{0.03668}{1.34} = 0.027$$

0.027 < 0.1 hence the matrix A is consistent, and the estimated weights shown in Table 3 can be used.

In this present study, CR < 0.1 hence the matrix A is consistent, and the estimated weights shown in Table 3 can be used.

Table 3: Assessments of probability for various parameter classes

Parameter	Feature/ Class	Unit	Rank	Normalized Weight (W)	Contribution to Ground water Recharge
Coefficient of Anisotropy	1 – 1.12		2		Low
	1.13 – 1.48		3	2.81	Moderate
	1.49 – 1.96		4		High
Aquifer Resistivity	0 – 90		1		Very Low
	91 – 150		2	0.95	Low
	151 – 250	Ωm	4		High
	251 – 489		3		Moderate
Aquifer Thickness	5 – 10	M	1		Very low
	11 – 15		2	0.73	Low
	16 – 20	-	3		Moderate
	21 – 29		4		High
Overburden Thickness	7 – 11		1		Very low
	12 – 16		2	1.23	Low
	17 – 21	m	3		High
	22 – 33		4		Moderate
Hydraulic Conductivity	0 – 0.012		1		Very Low
	0 013 – 0.024		2	0.28	Low
	0 025 – 0.036		3		Moderate
	0.037 – 0.048	m/s	4		High
Transmissivity	0 – 0.20				Very Low
	0.21 – 0.30	m^2/day	2	0.40	Low
	0.31 – 0.40				Moderate
	0.41 – 0.70				High
Storativity	0.000015 – 0.000030		1		Very Low
	0.000031 – 0.000045	psi^{-1}	2	0.55	Low
	0.000046 – 0.000058		3		Moderate
	0.000058 – 0.000085	-	4		High

3. Results and Discussion

3.1 Characteristic of the VES Curves

The H, HA, and KH are the major curve types delineated within the study area varying from three to four layers (Figure 3). Figure 4 shows the percentage range of the curve types with HA being the predominant

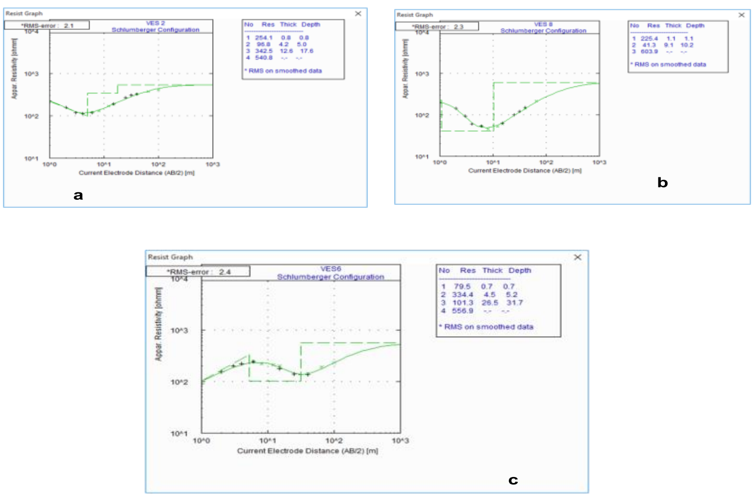

Figure 3: Typical Curve Types (a) HA (b) H (c) KH

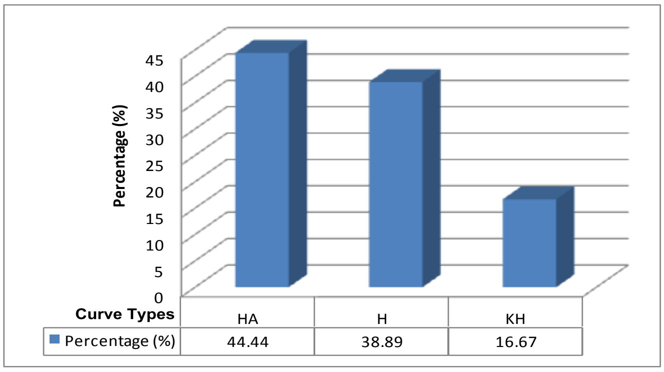

Figure 4: Percentage Range of the Curve Types

3.2 Geoelectric Sections

Figure 5 shows the geoelectric section along traverse one which comprises topsoil, weathered layer, fractured basement, and fresh basement. The topsoil resistivity values range from 183 to 518 Ωm with its thickness varying from 1 to 3.8 m, while the underlying layer has a resistivity value ranging from 35 to 97 Ωm which is indicative of a clayey/clayey sand horizon, with the thickness varying from 1.2 to 3.8 m The fractured basement is characterized by resistivity values ranging from 127 to 347 Ωm with layer thickness varying from 2 to 28 m, representing the Auriferous zone/water-bearing formation, beyond which is the crystalline bedrock with layer Resistivity varying from 450 to 743 Ωm. the weathered layer will serve as a protective capacity for the aquifer, especially VES 1.

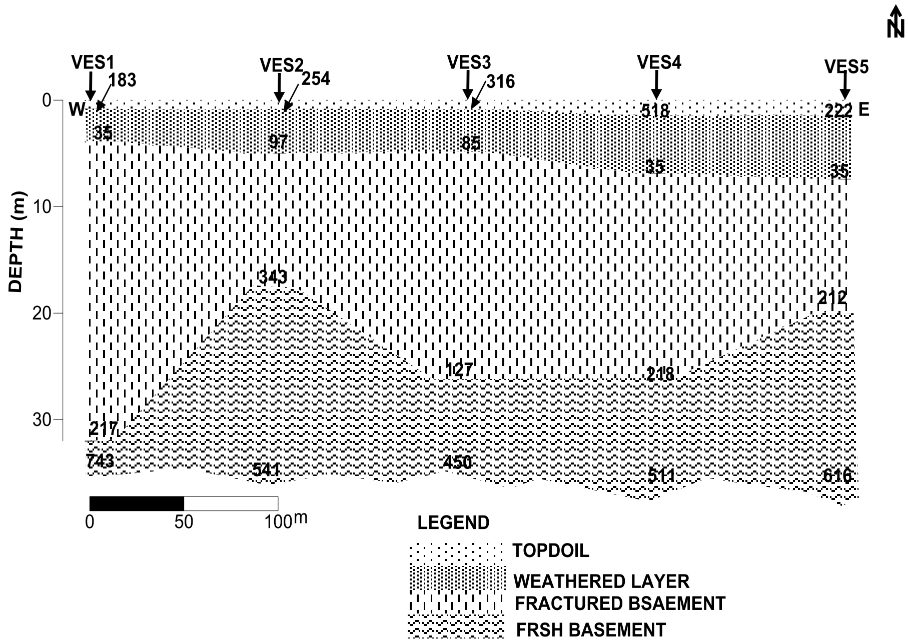

Figure 5: Geoelectric Section along Traverse One

The geoelectric section along Traverse two (Figure 6) comprises topsoil, weathered layer, fractured basement, and fresh basement. The Topsoil horizon has a resistivity variation of 60 to 614 Ωm with its thickness varying from 0.5 to 1.1 m, while the weathered layer has a resistivity value ranging from 31 to 334 Ωm with layer thickness ranging from 1 to 5 m. The fractured basement has a resistivity value ranging from 101 to 249 Ωm with its thickness varying from 5 to 35 m. This layer constitutes the aquiferous zones. VES 1, 6, 9, and 12 have an appreciable thickness and a high degree of fracturing which could be recommended for borehole drilling and wells. The fresh basement has a resistivity value ranging from 526 to 744 Ωm.

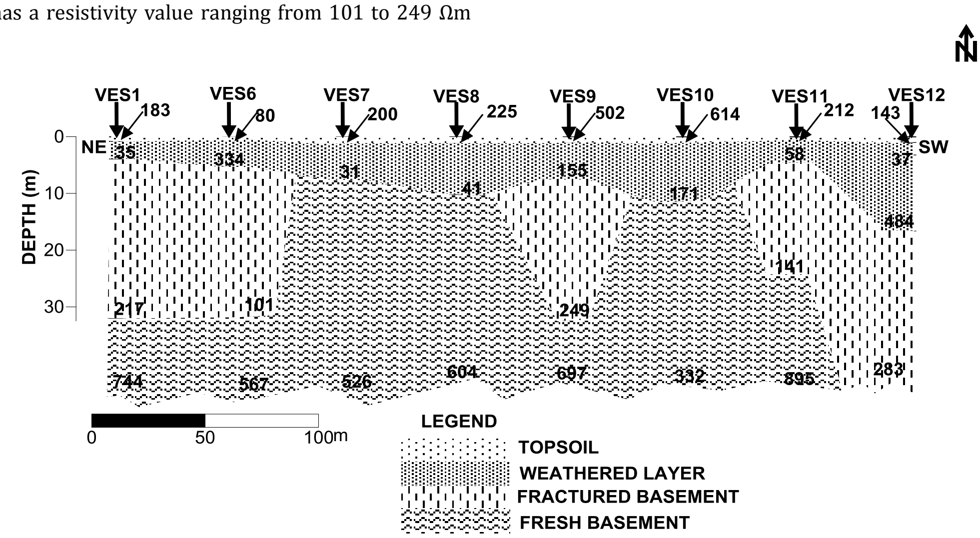

Figure 6: Geoelectric Section along Traverse Two

The Geoelectric section along Traverse three (Figure 7) comprises topsoil, clay, weathered layer, fractured basement, and fresh basement. The topsoil horizon has a thickness ranging from of 1to 2.2 m and layer resistivity ranging from 73 to 151 Ωm, indicative of clayey, clayey sand, and sandy clay materials, while the underlying layer constitutes the clayey formation with layers Resistivity ranging from 8 to 37 Ωm, with its thickness varying from 3 to 7.5 m. the weathered layer has a resistivity of 484 Ωm with thickness ranging from 4.3 to 15.9 m, while the fractured basement has a resistivity of 283 Ωm. Beyond this is the fresh basement with a layer of resistivity varying from 484 to 6034 Ωm. VES 12 is the only promising point for water sustainability, where a suspected fracture exists from 18 m beyond.

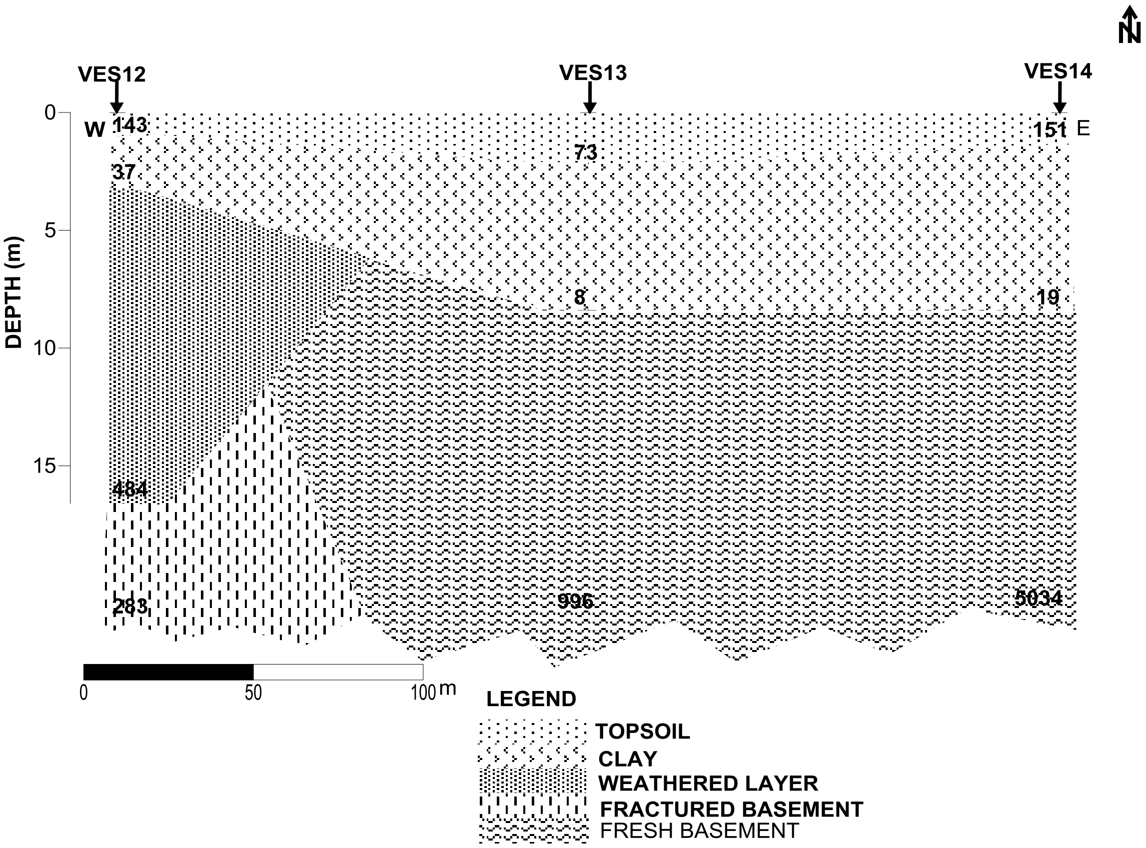

Figure 7: Geoelectric Section along Traverse Three

The Geoelectric section across Traverse 4 comprises three subsurface lithological layers; topsoil, weathered layer, and fresh basement (Figure 8). The topsoil has layer resistivity values ranging from 72 to 614 Ωm, indicative of clay, clayey sand, sandy, sand, and laterite, and its thickness ranges from 0. 8 to 1.2 m. The weathered layer has a resistivity value ranging from 12 to 171 Ωm and thickness values varying from 1.1 to 12.1 m, while the fresh Basement has a resistivity varying from 332 to 2848 Ωm. Hence, it offers little or no groundwater prospect. The recognizable structural feature in this section is the weathered layer. The weathered layer at VES10 could be a good prospect for groundwater. The total depth of VES10 will make it not suitable for borehole drilling but well is highly recommended.

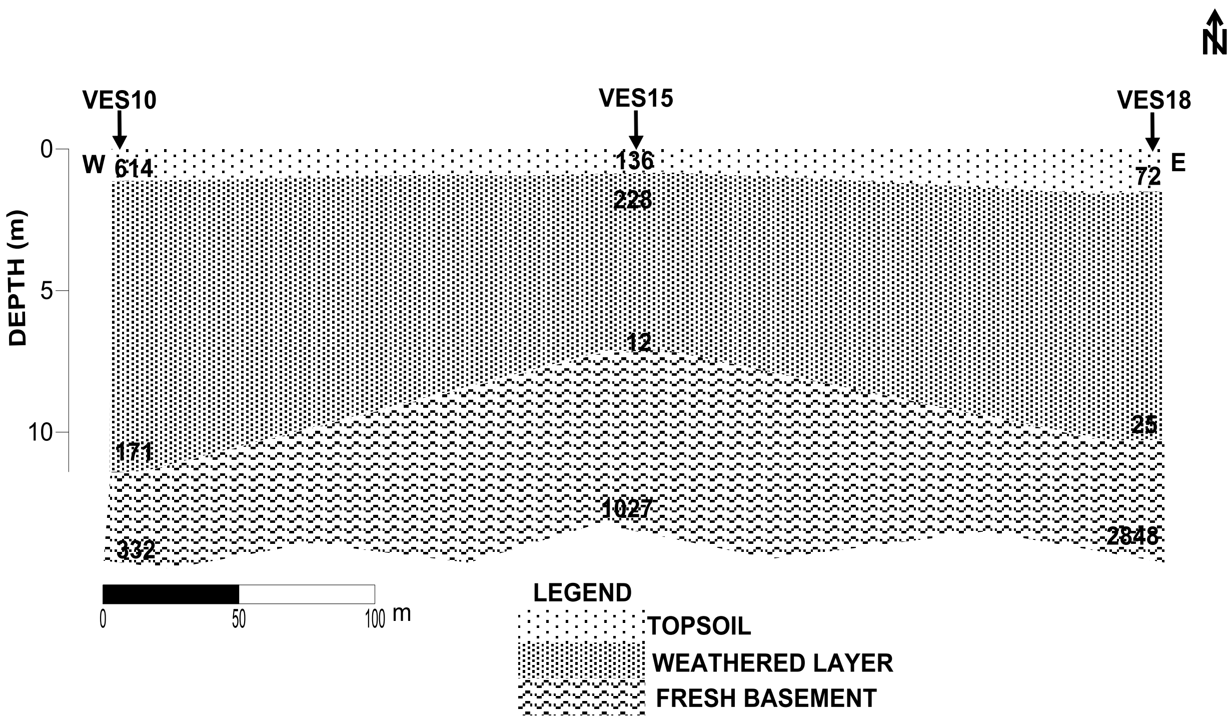

Figure 8: Geoelectric Section along Traverse Four

Figure 9 shows the geoelectric section along traverse five which comprises topsoil, weathered layer, fractured basement, and fresh basement. The topsoil has a layer Resistivity varying from 146 to 502 Ωm, while the thickness ranges from 0.5 to 1.4 m. The underlying weathered layer has layer Resistivity values ranging from 42 to 155 Ωm and thickness varied from 1.4 to 14 m. The third layer constitutes the fractured basement with a resistivity value of 249 Ωm and thickness tending to 35 m beneath VES9. The fourth layer is the fresh basement with resistivity value ranging from 692 to 1204 Ωm beneath VES9. The weathered layer is predominantly clayey. Hence, it offers little or no groundwater prospect. The recognizable structural feature in this section is the fracture. The fractured basement could be a good prospect for groundwater.

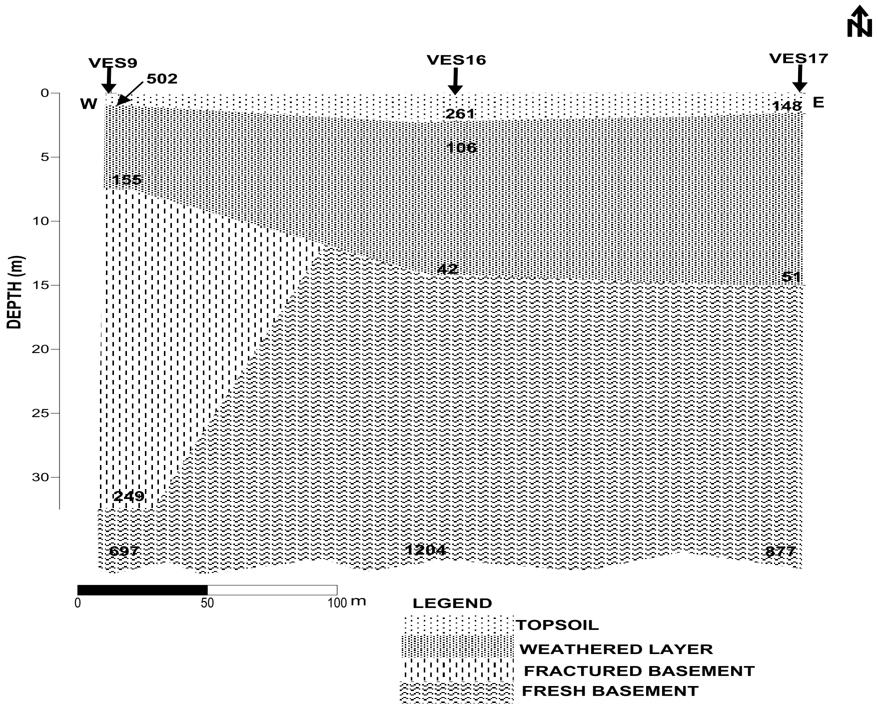

Figure 9: Geoelectric Section along Traverse Five

3.3 Geoelectric Maps

3.3.1 Aquifer Resistivity Map

Groundwater sustainability in a crystalline basement environment is anchored on several favorable geologic factors which include thick overburden, structural features, associated with a network of fractures, Crack rework of joints, highly weathered materials, and faults. This plays a major role in aquifer productivity or otherwise in this particular geologic environment. The aquifer resistivity map has a value ranging from 0 to 480 Ωm (Figure 10). Several factors may directly influence aquifer resistivity which requires a good understanding of the geologics and empowerment that enables good judgment and discretion in decision-making. Some of these include but are not limited to the nature of rock types, weathering history, and the nature of previous Techtronic activities. However, in this particular environment; extremely low aquifer resistivity may result from the influence of clayey materials, activities of fresh basement rocks, or highly resistivity geologic materials that may not be favourably to water sustainability in a basement complex environment. Therefore, the aquifer resistivity maps was categorized into four major controlling factors such as high, moderate, low, and very low. The high aquifer resistivity region has a value ranging from 400 to 480 Ωm. moderate aquifer resistivity region has a value ranging from 240 to 320 Ωm, Region of low aquifer resistivity has a value varying from 80 to 240 Ωm, while very low aquifer resistivity has a value varying from 0.0 to 80 Ωm. The information obtained indicates that the greater part of the study area, from the centers, up to the entire western end and rising towards the northern part of the study area with aquifer resistivity of between 80Ωm to 240Ωm holds the best prospect for water sustainability while the remaining part of the study area, hold the very lean prospect for water sustainability.

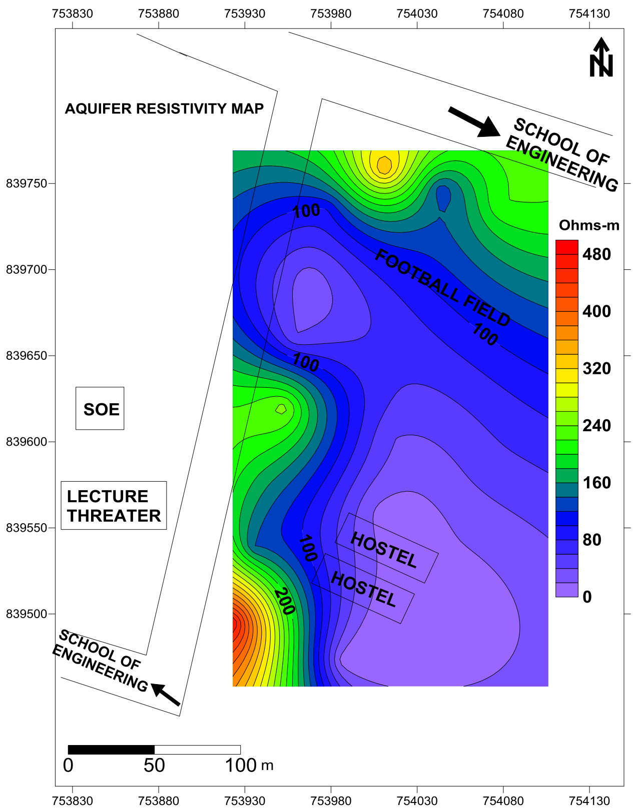

Figure 10: Aquifer Resistivity Map of the Study Area

3.3.2 Aquifer Thickness Map

Geologic dynamics allow for a direct relationship between aquifer thickness and water sustainability in a crystalline basement complex environment in such a way that the higher the aquifer thickness, the better the prospect for groundwater sustainability. The aquifer thickness values of the study area vary from 5 to 29 m (Figure 11). The Northwestern western, southwestern, and northeastern region with aquifer thickness values ranging from 17 to 29 m holds the greater prospect for water sustainability in the study area, while the south, southwestern southeastern, center, eastern, and northeastern parts with thickness values varying from 5 to 16.9 m has the low prospect for groundwater sustainability. Regions of high aquifer thickness indicate a high degree of groundwater accumulation within the region, especially if the aquifer formation has high permeability.

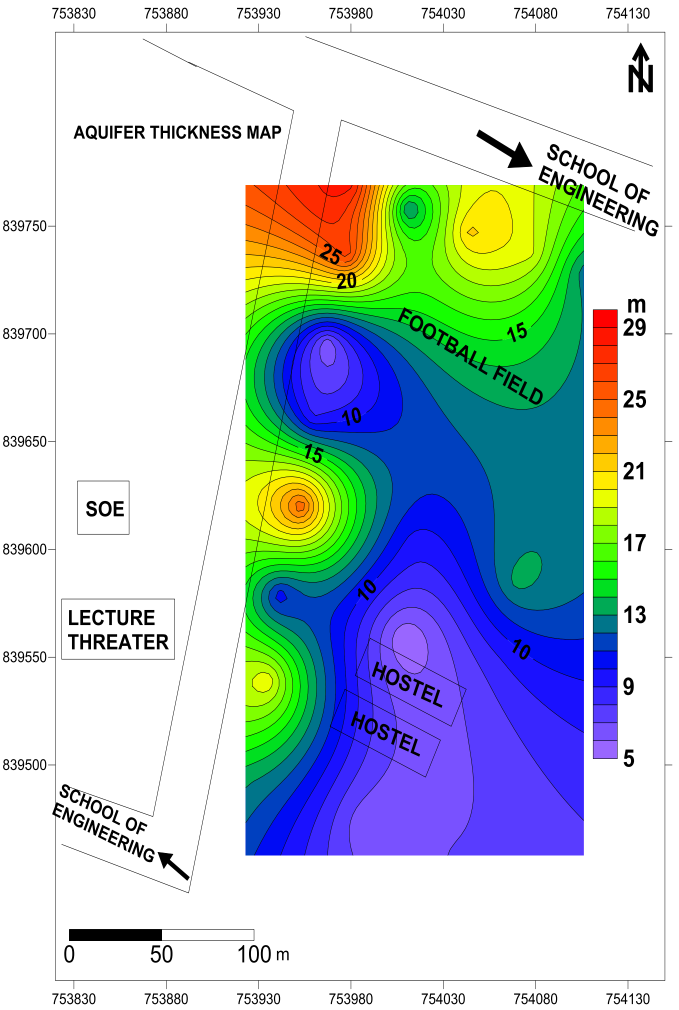

Figure 11: Aquifer thickness map of the study area

3.3.3 Overburden Thickness Map

Overburden thickness is one of the major controlling factors for groundwater sustainability in a crystalline basement environment. The summation of all the subsurface strata before the fresh basement for the Vertical Electrical Sounding (VES) points such as topsoil, weathered basement, and fractured basement was used to model the overburden thickness map. The summation of all the loose materials before the fresh basement is term overburden thickness (Olubusola *et al.,* 2023). High overburden thickness has a greater prospect for groundwater. Figure 12 shows the overburden thickness map varies from 7 to 31 m. The study area was categorized into three distinctive geologic regions such as high, moderate, and low. The high overburden thickness was observed at the northwestern, northeastern western, and southwestern regions with layer overburden thickness ranging from 19 to 31 m, depicting greater prospects for water sustainability in the study area. The moderate overburden thickness was found in the northeastern, southwestern, southeastern, and northwestern parts with values ranging from 12 to 18 m showing moderate prospect for groundwater sustainability, while low overburden thickness with values varying from 7 to 11 m was observed at the northwestern and southeastern regions of the study area indicative of low groundwater sustainability prospect.

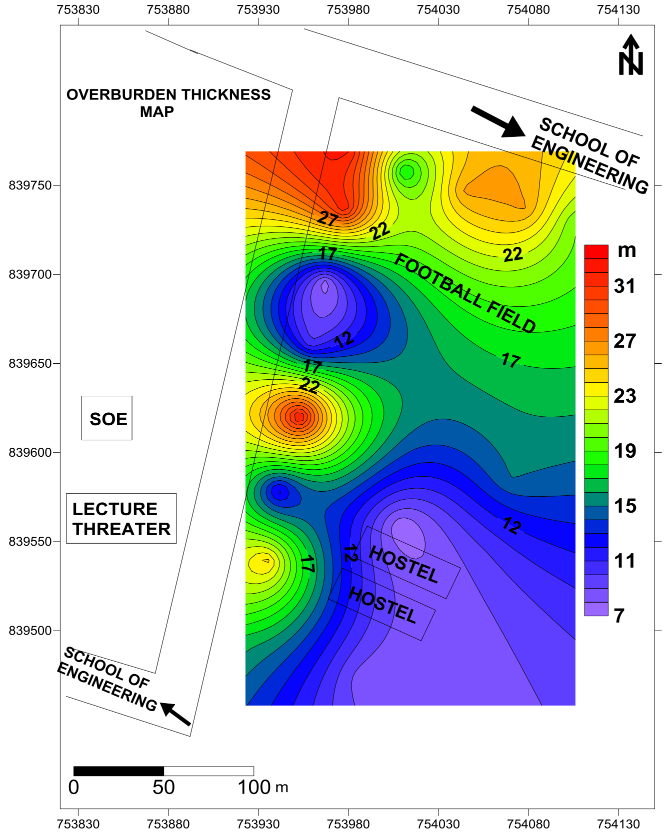

Figure 12: Overburden thickness map of the study area

3.4 Coefficient of Anisotropy

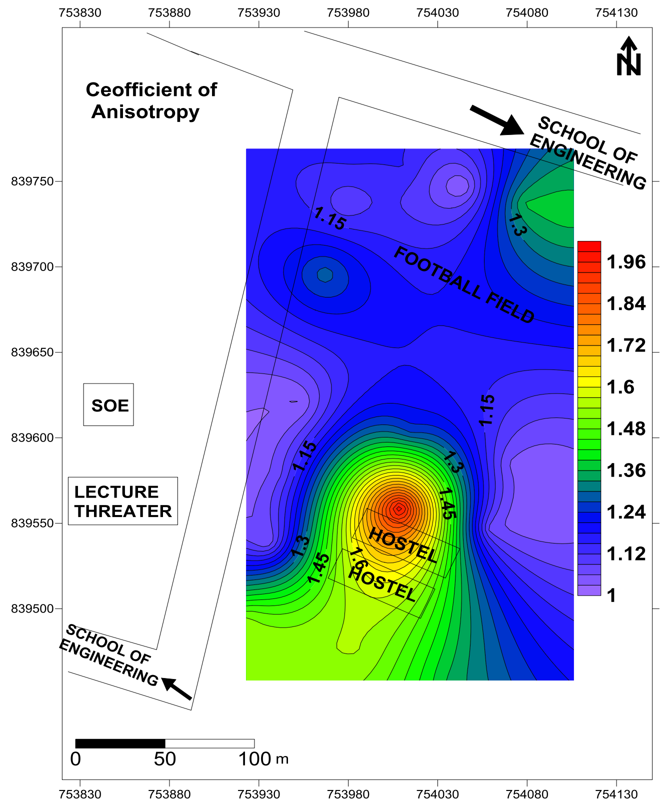

Figure 13: Coefficient of anisotropy of the study area

The coefficient of anisotropy is a function of the orientations, migration patterns, and direction of water flow within the water-bearing formations which are influenced by several geologic factors such as the nature, types, tectonic and weathering history of the crystalline rock with a direct impact on porosity and permeability. Figure 13 exhibits the coefficient of anisotropy map of the study area with values ranging from 1.0 to 1.96, which illustrates the extent of variation of anisotropy in rock formation. The areas with the high coefficient of anisotropy values ranged from 1.31

to 1.96 in the northeastern and southwestern parts. This is indicative that the extent of weathering and fracturing of the underlying rock formation having a high degree of groundwater accumulation range must have widened in all patterns, resulting in higher porosity (Bawallah et al. 2021a; Olubusola et al., 2023). However, unidirectional structures (fracture/fault) have a low record of groundwater accumulation due to the low coefficient of anisotropy observed in the northern, northeastern, eastern, southeastern, southern, southwestern, and northwestern regions with values ranging from 1 to 1.30 which occupied 95% of the study area.

3.5 Hydraulic Conductivity

Hydraulic conductivity measures the flow of water passing through soil or rock. It reflects the prolific nature of an Aquifer. Figure 14 shows the hydraulic conductivity map of the study area with values ranging from zero (0) to 0.054 m/s. High hydraulic conductivity has a value ranging from 0.040 to 0.054 m/s was observed at the southeastern and traces at the northwestern part of the investigated area, which indicates high permeable materials that allow easy flow of water. Moderate hydraulic conductivity was observed at the northwestern, central, southeastern, and southwestern regions of the study area with values ranging from 0.030 to 0.039 m/s; indicating of moderately permeable materials. The edges of western, southwestern, northwestern, and northeastern parts are characterized by low to very low hydraulic conductivity with values ranging from zero (0) to 0.029 m/s indicating low permeable materials. These regions are considered very poor in terms of groundwater yield and sustainability.

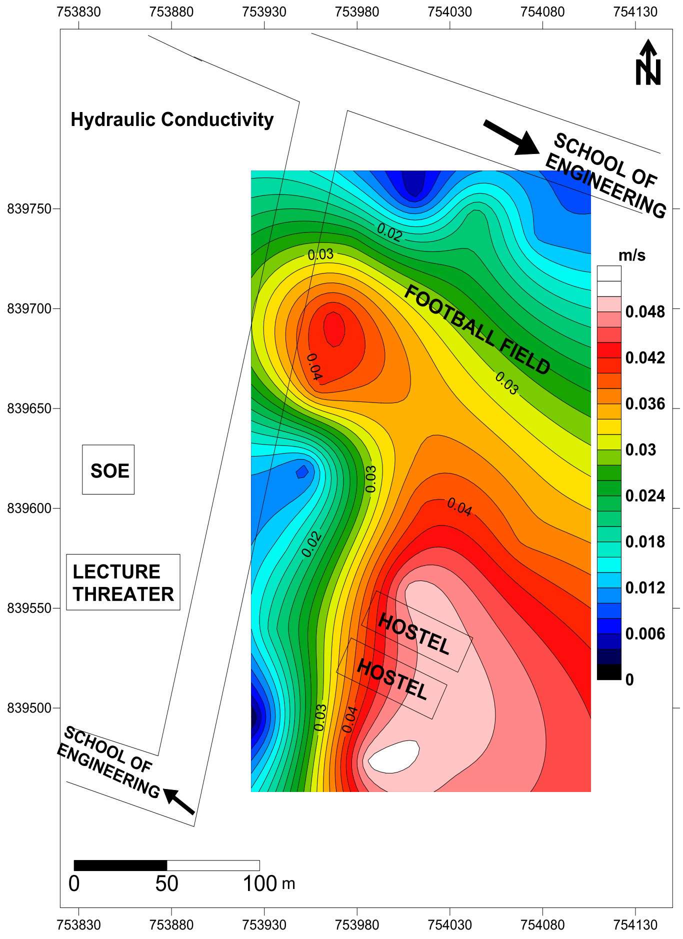

Figure 14: Hydraulic conductivity map of the study area

3.6 Transmissivity

This is a reflection of the water flow rate and rechargeability of an Aquifer in a water-bearing formation. The Transmissivity properties were categorized into low, medium, and high with values ranging from 0.0 to 0.2, 0.21-0.4, and 0.041 to 0.6 m/day (Figure 15). The low transmissivity was found at the edge of northeastern, northern, southwestern, and western parts of the study area indicating low groundwater prospect, while the medium transmissivity was observed at the northwestern, southwestern, western, southeastern, and central parts indicating moderate groundwater prospect. High Transmissivity was found as a small closure at the northwestern part indicating a high prospect for water sustainability.

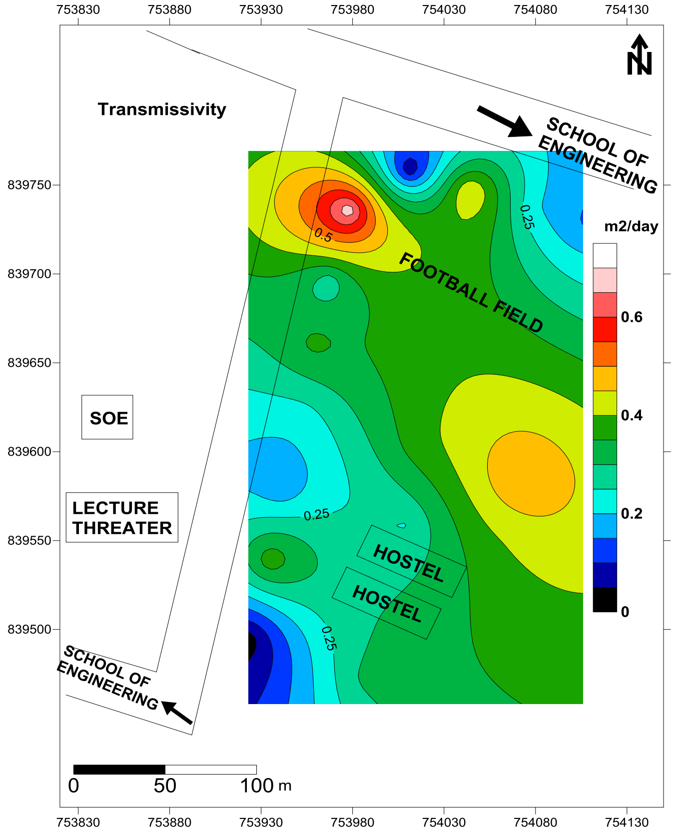

Figure 15: Transmissivity map of the study area

3.7 Storativity

Figure 16 shows the storativity map of the study area with values ranging from 1.5 x 10^{-5} to 8.5 x 10^{-5} psi^{-1}. The storativity map was categorized into high, medium, and low. The medium storativity aquifer zone was found at the edges of northeastern, northern, western, and southwestern parts with values ranging from 3.5 x 10^{-5} to 5.49 x 10^{-5} psi^{-1}, while low storativity occupied the entire southeastern, central, eastern, and some parts of southwestern, northwestern, and northeastern regions with a value ranging from 1.5 x 10^{-5} to 3.49 x 10^{-5} psi^{-1}.

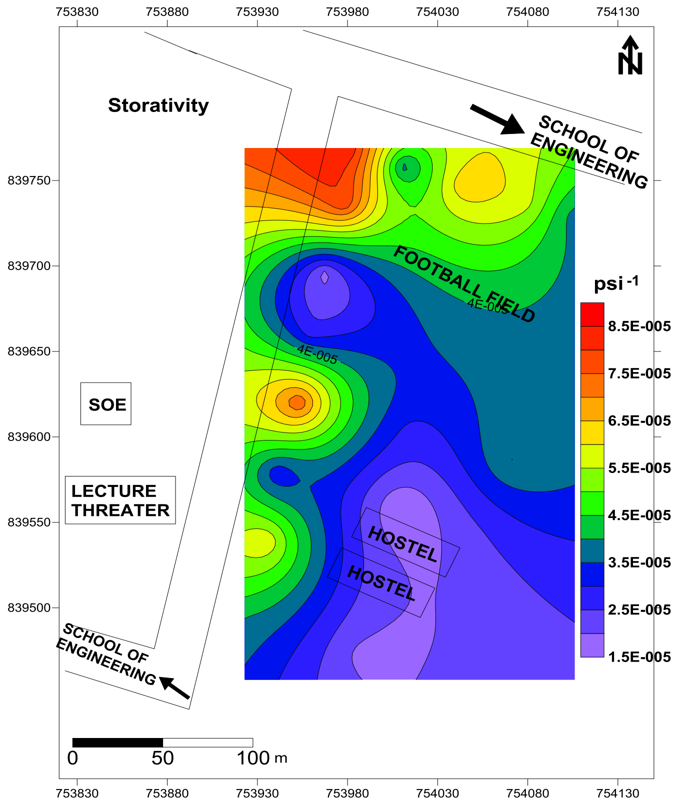

Figure 16: Storativity map of the study area

3.8 2D Resistivity Imaging

A 2-D imaging of the subsurface was also undertaken across Tr.1, 2, and 3, on an E-W orientation (Figure 17 a to c)); The information obtained, indicated, that Tr.1 is characterized by shallow overburden from about the middle towards the Eastern end of the Traverse, while a similar trend was observed towards the west end of Traverse two and three: making prospecting for groundwater more viable along Traverse 2 and 3 of the study area.

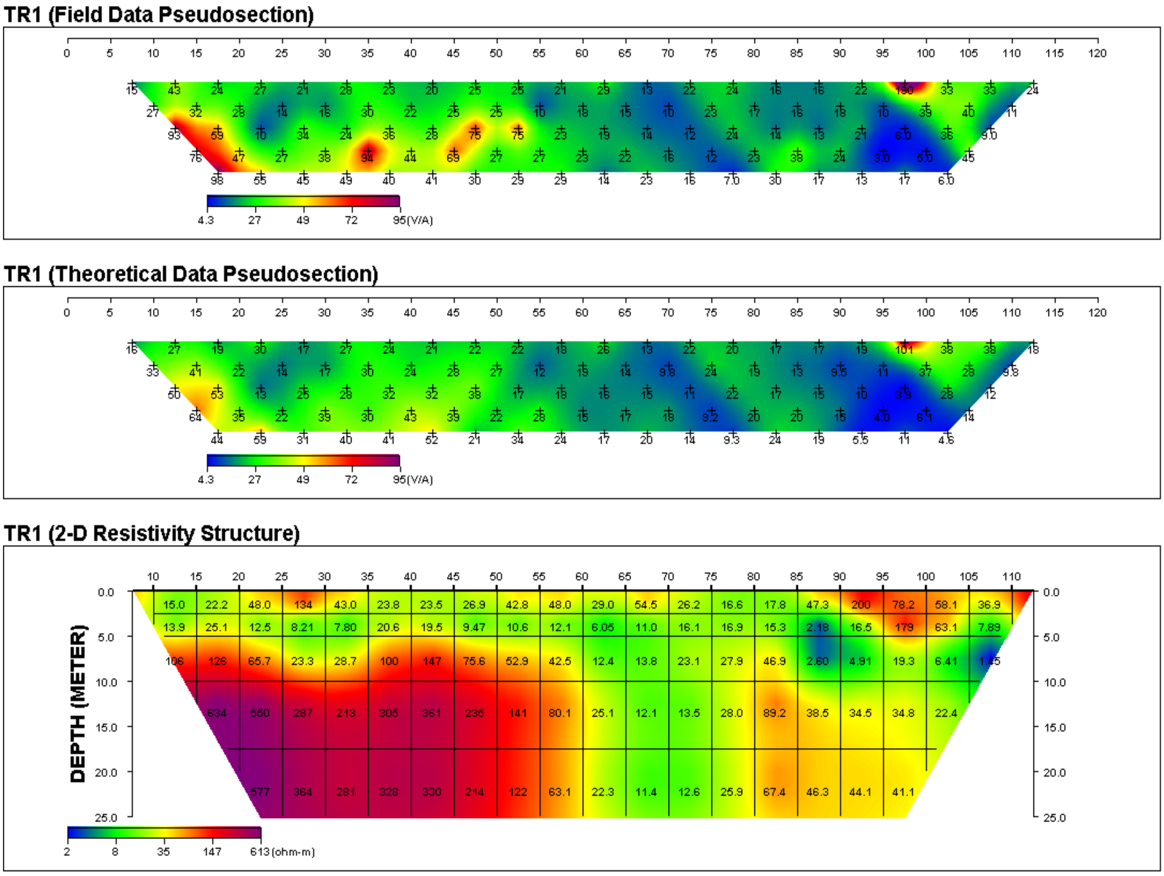

Figure 17a: 2D Resistivity Imaging along traverse one

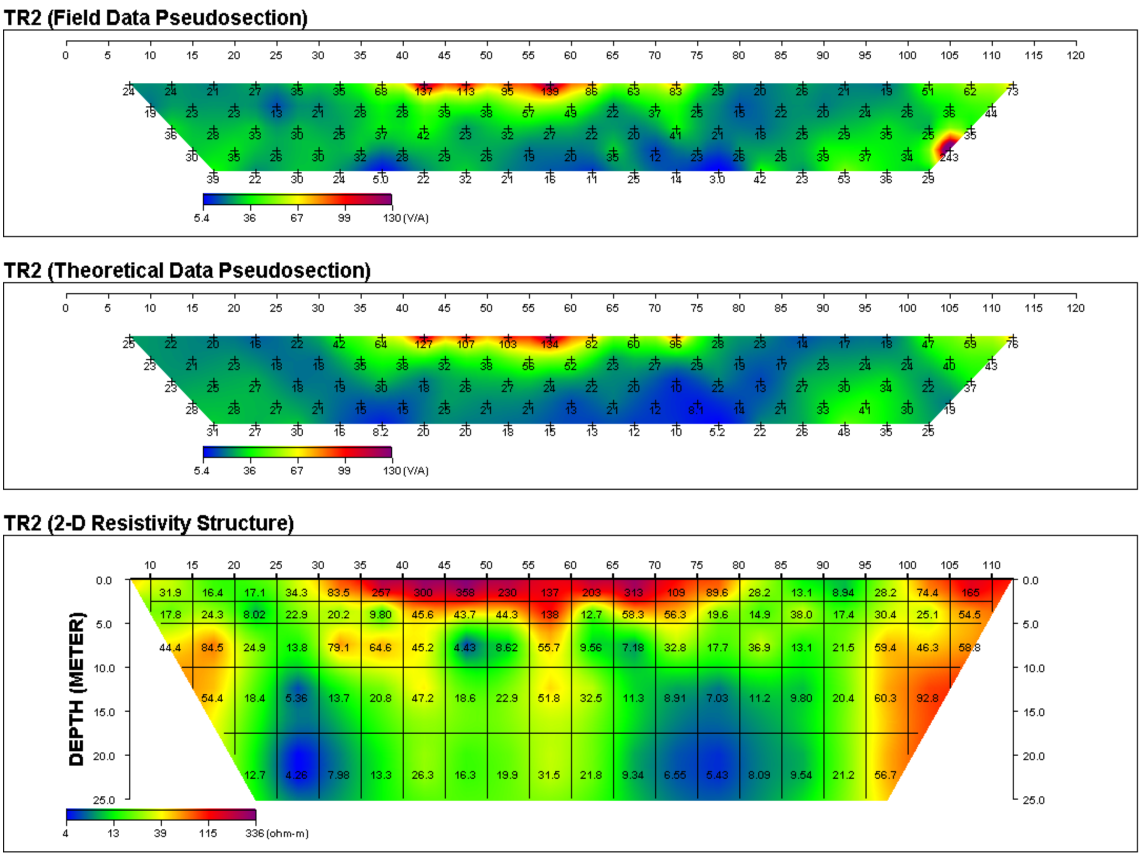

Figure 17b: 2D Resistivity Imaging along traverse two

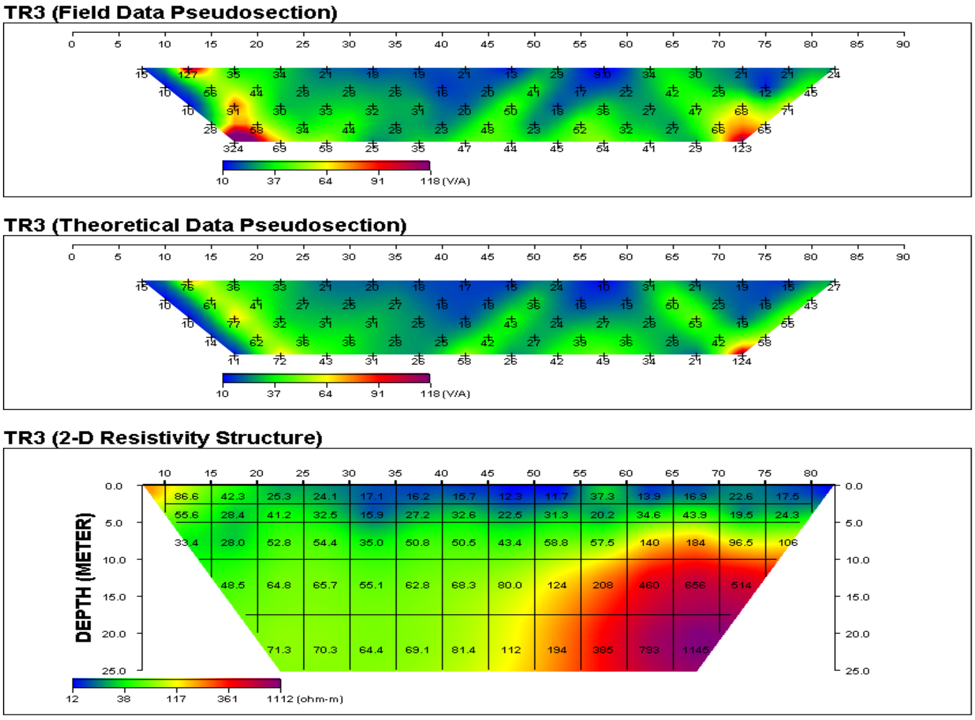

Figure 17c: 2D Resistivity Imaging along traverse three

3.9 Modeling of Groundwater Potential Map

In the study region, suitable places for borehole and well establishment were identified using electrical resistivity data and a geographic information system. Groundwater potential zones were identified using seven (7) geo-informative geoelectric maps, which are crucial for the storage and distribution of groundwater (Figure 18). The zones were then grouped into many distinctive classes. Appropriate weights were assigned to each category based on their respective influence on groundwater potential. The Surfer 12 platform's converting utilities were used to transform the Groundwater Potential Index (GPWI) values obtained into raster format after every theme layer's final weights had been determined. This map was generated from a combination of the entire controlling factor that surrounds groundwater productivity and sustainability in a typical crystalline Basement Complex region of Ado Ekiti based on the information obtained from the study location. The groundwater potential was characterized into four distinctive categories, namely; very low, low, moderate, and high groundwater potential. The southern, the southeastern, and the eastern end, upwards to the entire center part of the study area was identified to be of very low groundwater potentials and this contributes about 50% of the study area. Part of the Southwestern upwards to the centre, and towards the entire western and north western end, extended to the Eastern end of the study area was identified to be of low groundwater bearing potentials and occupied 27% of the study location. A trace at the northern and southwestern indicated high groundwater potential which occupied 6% of the study area, while the rest of the study area exhibited moderate groundwater potential which occupied 17% of the study location.

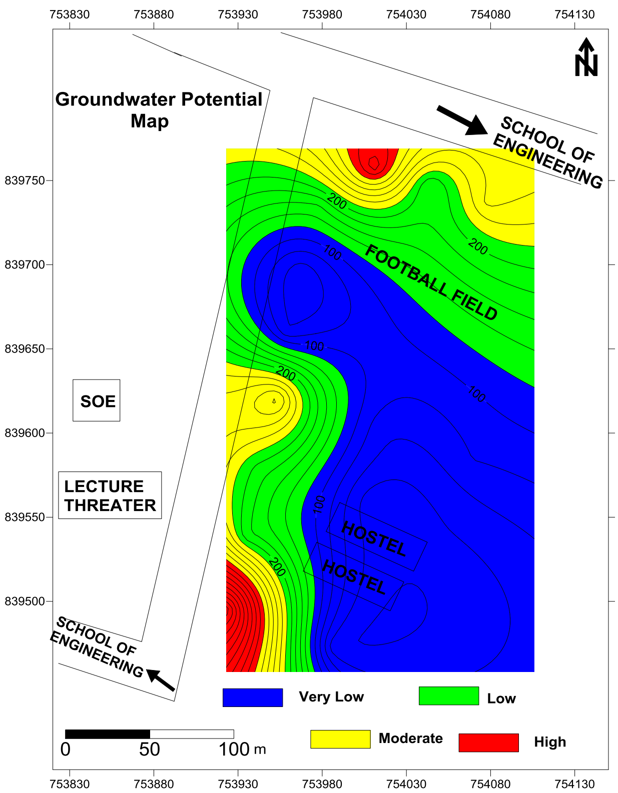

Figure 18: Groundwater Potential Map

4. Conclusion

This research work has been able to justify the tautology of electrical resistivity method and MCDA in the context of AHP in groundwater occurrence evaluation for decision policymakers in a crystalline basement complex of the Federal Polytechnic Ado Ekiti, Ekiti State, Nigeria. The hydrogeological investigation involved the extraction of geoelectric maps from the first and second-order parameters in the area. The depth-sounding data interpretation revealed three to four subsurface layers namely: the topsoil, weathered layer, fractured basement, and fresh basement.. In order to establish areas with potential for groundwater in parts of study area, the MCDA in the context of the AHP approach was used to integrate geoelectric parameters of multiple variables. Aquifer resistivity, aquifer thickness, coefficient of anisotropy, overburden thickness, hydraulic conductivity, storativity, and transmissivity were taken into consideration as the most crucial factors affecting groundwater control. However, weighted value determination was performed after each geoelectric map had been gathered because all the components do not have equal weight in influencing groundwater. The groundwater potential was characterized into four distinctive categories, namely; very low, low, moderate and high groundwater potential. The southern, the southeastern, and the eastern end, upwards to the entire center part of the study area was identified to be of very low groundwater potentials and this contributes about 50% of the study area. Part of the Southwestern upwards to the centre, and towards the entire western and north western end, extended to the Eastern end of the study area was identified to be of low groundwater bearing potentials and occupied 27% of the study location. A trace at the northern and southwestern indicated high groundwater potential which occupied 6% of the study area, while the rest of the study area exhibited moderate groundwater potential which occupied 17% of the study location. Considering the complex nature of a typical crystalline Basement complex, it is rather expedient that a multi-criteria decision-making approach should be adopted, to achieve the goal of water sustainability in rocky environment. The methodology adopted in these research findings can be replicated at the regional level.

Funding

This study did not receive any funding from governmental or non-governmental financial assistance to carry out this research.

References

Abijith, D., Saravanan, S., Singh, L., Jennifer, J.J., Saranya, T., Parthasarathy, K.S.S., 2020. GIS-based multicriteria analysis for identification of potential groundwater recharge zones - a case study from Ponnaniyaru watershed, Tamil Nadu, India. HydroResearch, https://doi.org/10.1016/j.hydres.2020.02.002.

Abu El-Magd, S.A., Embaby, A., 2021. To investigate groundwater potentiality, a GIS-based model was integrated with remote sensing data in the Northwest Gulf of Suez (Egypt). Arab. J. Geosci., 14, 2737.DOI:10.1007/s12517-021-08396-

Adebiyi, A.D., Ilugbo, S.O., Bamidele, O.E., Egunjobi, T., 2018. Assessment of aquifer vulnerability using multi- criteria decision analysis around akure industrial estate, Akure, Southwestern Nigeria. J Eng Res Rep 3(3): Pp. 1–13

Adebo, B.A., Ilugbo, S.O., Jemiriwon, E.T., Ali, A.K., Akinwumi, A.K., Adeniken, N.T., 2022 Hydrogeophysical Investigation Using Electrical Resistivity Method within Lead City University Ibadan, Oyo State, Nigeria. Int J Earth Sci Knowl Appl 4(1): Pp. 51–62

Adebo, B.A., Layade, G.O., Ilugbo, S.O., Hamzat, A.A., Otobrise, H.K., 2019. Mapping of subsurface geological structures using ground magnetic and electrical resistive ty methods within lead city university Southwestern Nigeria. Kada J Phys 2(2): Pp. 64–73

Adebo, A.B., Ilugbo, S.O., Oladetan, F.E., 2018. Modeling of groundwater potential using Vertical Electrical Sounding (VES) and multi-criterial analysis at Omitogun Housing Estate, Akure, Southwestern Nigeria. Asian J Adv Res Rep 1(2): Pp. 1–11

Aggarwal, M., Saravanan, S., Jennifer, J.J., Abijith, D., 2019. Delineation of groundwater potential zones for hard rock region in Karnataka using AHP and GIS. In: Advances in Remote Sensing and Geo Informatics Applications. Springer, Cham, Pp. 315–317. DOI: 10.1007/978-3-030-01440-7_71

Akintorinwa, O.J., Atitebi, M.O., Akinlalu, A.A., 2020. Hydrogeophysical and aquifer vulnerability zonation of a typical basement complex terrain: A case study of Odode Idanre southwestern Nigeria. Heliyon, 6, Pp. e04549

Akinluyi A.O., Olorunfemi M.O., Bayowa, O.G., 2021. Application of remote sensing, GIS and geophysical techniques for groundwater potential development in the crystalline basement complex of Ondo State, Southwestern Nigeria. Sustainable Water Resources Management, 7(4), Pp. 1-15. https://doi. org/10. 1007/s40899-020-00486-5

Akinluyi F.O., Olorunfemi M.O., Bayowa O.G., 2018. Investigation of the influence of lineaments, lineament intersections and geology on groundwater yield in the basement complex terrain of Ondo state, Southwestern Nigeria. Appl Water Sci. https:// doi. org/ 10.1007/ s13201- 018- 0686-x

Akintorinwa, O.J., Atitebi M.O., and Akinlalu, A.A., 2020. Hydrogeophysical and aquifer vulnerability zonation of a typical basement complex terrain: a case study of OdodeIdanre Southwestern Nigeria. Heliyon. https:// doi. org/ 10.1016/j. heliy on.2020. e04549

Al-Djazouli, M.O., Elmorabiti, K., Rahimi, A., Amellah, O., Fadil, O.A.M., 2020. Delineatin gofgroundwater potential zones based on remote sensing, GIS and analytical hiera rchical process: a case of Waddai, eastern Chad. Geo J. https:// doi. org/ 10. 1007/ s1070 802010160-0

Aluko, A.B., 2008. Geology of Akure Area Southwestern Nigeria. Unpublished B.Tech. Thesis, Federal University of Technology, Akure, 70.

Anusha, B.N., Babu, K.R., Kumar, B.P., Kumar, P.R., Rajasekhar, M., 2022. Geospatial approaches for monitoring and mapping of water resources in semi-arid regions of Southern India. Environ. Challenges,8,100569. doi:10.1016/j.envc.2022.1005 6 9.

Arshad, A., Zhang, Z., Zhang, W., Dilawar, A., 2020. Mapping favorable groundwater potential recharge zones using a GIS-based analytical hierarchical process and probability frequency ratio model: a case study from an agro-urban region of Pakistan. Geoscience Frontiers 11 (5), Pp. 1805–1819. https://doi.org/10.1016/j. gsf.2 01 9.12.013.

Boobalan, C., gurugnanam, B., 2016. Mapping of ground water potential zones in Sarabanga sub-basin, Cauvery River, South India using remote sensing and GIS techniques. Indian J. Appl. Res. 6 (2), 364-369.

Bawallah, M.A., Adiat, K.A.N., Akinlalu, A.A., Ilugbo, S.O., Akinluyi, F.O., Ojo, B.T., Oyedele, A.A., Bamisaye, O.A., Olutomilola, O.O., Magawata, U.Z., 2021a Resistivity contrast and the phenomenon of geophysical anomaly in ground water exploration in a crystalline basement environment Southwestern Nigeria. Int J Earth Sci Knowl Appl 3(1): Pp. 23–36

Bawallah, M.A., Adiat, K.A.N., Akinlalu, A.A., Ilugbo, S.O., Akinluyi, F.O., Benjamin, O.O., Oyedele, A.A., Omosuyi, G.O., Aigbedion, I., 2021b. Groundwater sustainability and the divergence of rock types in a typical crystalline basement complex region Southwestern Nigeria. Turkish J Geosci 2(1): Pp. 1–11. https:// doi. org/ 10. 48053/ turkg eo. 777217

Bawallah, M.A., Ilugbo, S.O., Aina, A.O., Olufemi, B., Akinluyi, F.O., Ojo, B.T., Oyedele, A.A., Olasunkanmi, N.K., 2020a. Hydrogeophysical studies of central Kwara state basement complex of Nigeria. Int J Earth Sci Knowl Appl 2(3): Pp. 146–164

Bawallah, M.A., Ofomola, M.O., Ilugbo, S.O., Aina, A.O., Olaogun, S.O., Olayiwola, K.O., Awoniran, D.R., 2020b. Effect of Lineament and drainage orientation on groundwater potential of moroarea central Kwara state Nigeria. Indian J Sci Technol 13(10):Pp. 1124–1134

Bawallah, M.A., Adebayo, A., Ilugbo, S.O., Olufemi, B., Alagbe, O.A., Olasunkanmi, K.N., 2018a. Evaluation of groundwater prospect in a clay dominated environment of central Kwara state Southwestern Nigeria. Int J Adv Eng Res Sci 5(6): Pp. 45–56

Bawallah, M.A., Aina, A.O., Ilugbo, S.O., Ozegin, K.O., Olasunkanmi, K.N., 2018b. Evaluation of groundwater yield capacity using darzarrouk parameter of central Kwara state, Southwestern Nigeria. Asian J Geol Res 1(1):Pp. 1–13

Dippro for Windows Dippro TM Version 4.0 Processing and Interpretation software for Dipole Dipole electrical resistivity data. KIGAM, Daejon, South Korea; 2000.

Fadhilah, A., Suhailan, S., Yazid, M.S.M., Hasni, H., and Fatimah, G., 2011. Instant messaging and guided AHP for human resource selection. In: International Conference on Future Information Technology, IPCSIT. IACSIT Press, Singapore

Feizizadeh, B., Jankowski, P., Blaschke, T., 2014. A GISbased spatially-explicit sensitivityand uncertainty analysis approach for multi-criteria decision analysis. Computers and Geosciences, 64, Pp. 81-95.

Ilugbo, S.O., Adebiyi, A.D., 2017. Intersection of Lineaments for groundwater prospect analysis using satellite remotely sensed and aeromagnetic dataset around Ibodi, Southwestern Nigeria. Int J of Phys Sci 12(23): Pp. 329–353

Ilugbo, S.O., Ozegin, K.O., 2018a. Significances of Deep Seated Lineament in Groundwater Studies around Ilesha, Southwestern Nigeria. Asian J Geol Res 1(1): Pp. 1–16

Ilugbo, S.O., Adebiyi, A.D., Olomo, K.O., 2018b. Modeling of groundwater yield using gis and electrical resistivity method in a basement complex terrain, Southwestern Nigeria. J Geog EnvironEarth Sci Intern 16(1):Pp. 1–17

Ilugbo, S.O., Adebo, B.A., Olomo, K.O., Adebiyi, A.D., 2018c. Application of Gis and multi criteria decision analysis to geoelectric parameters for modeling of groundwater potential around ilesha, Southwestern Nigeria. Eur J Acad Essays 5(5):Pp. 105–123

Ilugbo, S.O., Edunjobi, H.O., Alabi, T.O., Ogabi, A.F., Olomo, K.O., Ojo, O.A., Adeleke, K.A., 2019. Evaluation of Groundwater Level Using Combined Electrical Resistivity Log with Gamma (Elgg) around Ikeja, Lagos State, Southwestern Nigeria. Asian J Geol Res 2(3):Pp. 1–13

Ilugbo, S.O., Adewoye, O.E., Aladeboyeje, A.I., Magawata, U.Z., Oyedele, A.A., Alabi, T.O., Owolabi, D.T., Adeleke, K.A., Adebayo, S.O., 2020. Modeling of groundwater potential using remotely sensed data within Akure metropolis Ondo State Southwestern Nigeria. Applied J Phys Sci 2(3):Pp. 38–54. https:// doi. org/ 10. 31248/ AJPS2 019. 028

Ilugbo, S.O., Aigbedion, I., and Ozegin, K.O., 2023. Structural mapping for groundwateroccurrence using remote sensing and geophysical data in Ilesha Schist Belt, Southwestern Nigeria, Geology, Ecology, and Landscapes, https://doi. org/10.1080/24749508.2023.2182063

Kardi, T., 2006. Analytic Hierarch Process (AHP) Tutorial http://people.revoledu.com/kardi/ tutorial /ahp/ (accessed on the 10th June, 2009).

Mohammadi-Behzad, H.R., Charchi, A., Kalantari, N., Nejad, A.M., Vardanjani, H.K., 2019. Delineation of groundwater potential zones using remote sensing (RS), geographical information system (GIS) and analytic hierarchy process (AHP) techniques: A case study in the Leylia–Keynow watershed, southwest of Iran Carbonates Evaporites 34, 13071319.

Olarewaju, V.O., 1988. REE in charnockitic and associated granitic rocks of Ado-Ekiti Akure, Southwest Nigeria: In: Precambrian Geology of Nigeria. (Edited by the Nigerian Geological Survey), Pp. 231-239.

Olorunfemi, M.O., 2008. Voyage on the skin of the earth: a geophysical experience. Inaugural lecture series 211. Obafemi Awolowo University, Ife

Olubusola, I. S., Isaac, A., Oyamenda, O. K., Adesola, B. M., 2023. Assessment of groundwater occurrence in a typical schist belt region in Osun State, Southwestern Nigeria using VES, aeromagnetic dataset, remotely sensed data, and MCDA approaches. Sustainable Water Resources Management, *9*(1). https:// doi.org/10.1007/s40899-02200810-1

Ozegin, K. O., Ilugbo, S. O., Ogunseye, T. T., 2023. Groundwater exploration in a landscape with heterogeneous geology: An application of geospatial and analytical hierarchical process (AHP) techniques in the Edo north region, in Nigeria. Groundwater for Sustainable Development, 20, 100871. https:// doi.org/10.1016/ j.gsd. 2022.100871

Pande, C.B., Moharir, K.N., and Singh, S.K., 2022. Groundwater flow modeling in the basaltic hard rock area of Maharashtra. India Appl Water Sci 12:12. https:// doi. org/ 10. 1007/ s13201021- 01525-y

Paul, R. S., Rawat, U., Sengupta, D., Biswas, A., Tripathi, S., Ghosh, P., 2020. Assessment of groundwater potential zones using multi-criteria evaluation technique of Paisuni River Basin from the combined state of Uttar Pradesh and Madhya Pradesh, India. Environmental Earth Sciences 79, Pp. 340. DOI: 10.1007/s12665-020-09091-3.

Raje, D., Mujumdar, P.P., 2010. Hydrologic drought prediction under climate change: Uncertainty modeling with Dempster-Shafer and Bayesian approaches. Advances in Water Resources. 33, Pp. 1176 – 1186.

Rahaman, M.A., Oluyide, P.O., Mbonu, W.C., Ogezi, A.E., Egbuniwe, I.G., Ajibade, A.C., Umeji, A.C., 1988. Recent advances in the study of the basement complex of Nigeria. In Precambrian Geology of Nigeria. Geological Survey of Nigeria Special Publication 11, 41.

Saaty, T.L., 1980. The analytic hierarchy process: planning, priority setting, resource allocation. McGraw-Hill, New York.

Saranya, T., Saravanan, S., 2020. Groundwater potential zone mapping using analytical hierarchy process (AHP) and GIS for Kancheepuram District, Tamilnadu, India. Model. Earth Syst. Environ. 6, Pp. 1105–1122.

Sengupta, D., Biswas, A., Ghosh, P., Rawat, U., Tripathi, S., 2021. Delineation of groundwater potential zones, groundwater estimation and recharge areas from Mahoba district of Uttar Pradesh, India. International Journal of Environmental Science and Technology 19, Pp. 12145-12168. DOI: 10.1007/s13762-021-03795-0.

Tanveer, D., Nachiketa, R., Adil, B., 2020. Delineation of potential groundwater recharge zones using analytical hierarchy process (AHP). Geology, Ecology, and Landscapes Pp. 1–16. https://doi.org/10.1080/24749508.2020.1726562.

Tolche, A.D., 2021. Groundwater potential mapping using geospatial techniques: a case study of Dhungeta-Ramis sub-basin, Ethiopia. Geol. Ecol. Landscape. 5 (1), Pp. 65-80. https://doi.org/10.1080/24749508.2020.1728882.

Vander Velpen, B.P.A., 2004. WinRESIST Version 1.0 Resistivity Depth Sounding Interpretation Software. M.Sc. Research Project, ITC, Delf Netherland.